Ultrasonics Sonochemistry 26 (2015) 48–55

Contents lists available at ScienceDirect

Ultrasonics Sonochemistry

journal homepage: www.elsevier.com/locate/ultson

Modification of foaming properties of soy protein isolate by high ultrasound intensity: Particle size effect

Rocío Morales, Karina D. Martínez *, Víctor M. Pizones Ruiz-Henestrosa, Ana M.R. Pilosof

Departamento de Industrias, Facultad de Ciencias Exactas y Naturales, Universidad de Buenos Aires, Ciudad Universitaria, 1428 Buenos Aires, Argentina

ARTICLE INFO

Article history:
Received 4 September 2013
Received in revised form 10 November 2014
Accepted 9 January 2015
Available online 17 January 2015

Keywords:
Soy protein isolate
Foaming properties
Interfacial properties
Ultrasound

ABSTRACT

The effect of high intensity ultrasound (HIUS) may produce structural modifications on proteins through a friendly environmental process. Thus, it can be possible to obtain aggregates with a determined particle size, and altering a defined functional property at the same time.

The objective of this work was to explore the impact of HIUS on the functionality of a denatured soy protein isolate (SPI) on foaming and interfacial properties. SPI solutions at pH 6.9 were treated with HIUS for 20 min, in an ultrasonic processor at room temperature, at 75, 80 and 85 °C. The operating conditions were: 20 kHz, 4.27 ± 0.71 W and 20% of amplitude. It was determined the size of the protein particles, before and after the HIUS treatment, by dynamic light scattering. It was also analyzed the interfacial behavior of the different systems as well as their foaming properties, by applying the whipping method.

The HIUS treatment and HIUS with temperature improved the foaming capacity by alteration of particle size whereas stability was not modified significantly. The temperature of HIUS treatment (80 and 85 °C) showed a synergistic effect on foaming capacity. It was found that the reduction of particle size was related to the increase of foaming capacity of SPI. On the other hand, the invariable elasticity of the interfacial films could explain the stability of foams over time.

1. Introduction

Proteins due to their amphiphilic character can adsorb at fluid interfaces. The adsorption of proteins at interfaces and other dynamic surface properties – such as film viscoelasticity – are known to play an important role in the formation and stability of food dispersed systems as foams and emulsions [1]. Because of the adsorption at fluid interfaces, protein molecules prevent the recoalescence of previously created bubbles or droplets. In addition, during the protein adsorption the surface or interfacial tension of the air–water or/and oil–water interface decreases which is an important attribute to optimize the input of energy involved in the foaming or emulsification process [2] and for the production of smaller bubbles or droplets, which is an important factor for the stability of the dispersions.

The use of soy proteins as functional ingredients in food manufacturing is increasing because of their role in human nutrition and health. The major globulins of soy protein are conglycinin (7S) and glycinin (11S). Native soy, because of its quaternary and compact tertiary structure, has limited foaming [3,4] and emulsifying [3,5] properties. Structural modifications by chemical methods such as deamidation, succinilation, reduction or denaturation, allow a greater conformational flexibility of the protein, which may improve its surface behavior and functionality [6,7]. The application of HIUS to modify biopolymers is being increasingly studied. Several works have focused on the ability of ultrasound to depolymerise polysaccharides such as dextran, xanthan, lambda-carrageenan, chitosan and starch [8–13], which impacts directly on their functional properties. Others authors [11] have demonstrated that ultrasonic radiation offers important potential for the conversion of biomass raw materials, such as polymeric carbohydrates, to useful lower molecular weight particles. In a previous publication [14] we succeeded in controlling the particle size with HIUS by combining different treatment times, temperatures and concentrations of whey protein isolate (WPI) solutions or gels. Other authors [15] could achieve a reduction in viscosity and an improvement in gelling properties of reconstituted WPC, whey protein retentate, milk protein retentate and calcium caseinate by sonication in pilot scale reactors.

The effect of ultrasound is related to cavitation, heating, dynamic agitation, shear stresses, and turbulence [16]. It may cause chemical and physical changes producing aggregates through covalent and non-covalent bonds by cyclic generation and collapse of

* Corresponding author. Tel.: +54 1145763377.
E-mail address: karinamartinez@di.fcen.uba.ar (K.D. Martínez).

http://dx.doi.org/10.1016/j.ultsonch.2015.01.011
1350-4177/

cavities. Thus, it is possible to obtain a determined aggregate particle size, leading to a defined functional property change.

Moreover, in the present work, a controlled denatured SPI was produced by heat treatment, enhancing the foaming properties as compared to native soy protein, but while maintaining an acceptable solubility compared to that found normally in commercial isolated soy protein [17]. Additionally, the HIUS treatment would modify the structure of the aggregates by improving the soy protein functionality.

The objective of this work was to determine the modifications of the foaming and interfacial properties in relation to the particle size of a denatured SPI applying HIUS, a clean and sure technique.

2. Materials and methods

2.1. Denatured soy protein production

Native soy protein isolate was prepared at 10:1 in water:protein from defatted soybean flour (Sanbra S.A., Brazil) by extraction at pH 8.0 with NaOH 0.25 M at room temperature during 1 h. It was centrifuged at 2100 rpm for 30 min and the supernatant was precipitated at pH 4.5 with HCl 3 M. It was again centrifuged at 2100 rpm for 30 min to obtain the precipitated protein fraction that was washed two times by the above procedure. After that, it was neutralized with NaOH 0.25 M at pH 7.0 and freeze-dried at room temperature during 48 h in a Stokes Mc Load Gage equipment. The protein content was 90.5% by Kjeldahl analysis, (Kjeltec Auto Analyzer 1030, Tecator, Sweden).

Denatured soy protein isolate (SPI) was prepared by heating a 50 g/l aqueous dispersion of the native soy protein isolate at 100 °C for 30 min. Then it was freeze-dried at room temperature during 48 h. Soy protein solubility was not affected by thermal treatment, being both native and denatured SPI 98% soluble [6].

2.2. Differential scanning calorimetry (DSC)

Differential scanning calorimetry was used to determine the onset (T_{onset}) temperature, the peak temperature (T_p), and the endset temperature (T_{end}) for HIUS-treated and control protein dispersions. A Mettler TA4000 Thermal Analysis System equipped with TA72 software (Schwerzenbach, Switzerland) was used. The instrument was calibrated with indium (156.6 °C), lead (327.5 °C) and zinc (419.6 °C). The thermal parameters were determined by heating 15–20 mg at 12% w/w of each sample from 0 to 95 °C at 10 °C/min. An empty pan was used as reference. The average value of at least two replicates was reported. The calorimetric thermogram showed that SPI was 100% denatured.

2.3. Solubility

A previous procedure [18] was used. Briefly, samples prepared at 2% wt, were centrifuged at 10,000 rpm for 30 min at room temperature. The supernatant containing the total soluble fraction was freeze-dried for 48 h in a Stokes equipment (Barber-Colman, Philadelphia, PA 19120, USA), operating at 40 °C condenser plate temperature and a chamber pressure of less than 100 mmHg. Then, samples were weighted and solubility was expressed as:

$$S\ \% = (\text{total soluble solids(g)}/\text{total solids(g)}) \times 100 \quad (1)$$

2.4. Foaming properties

2.4.1. Foam formation

Solutions at 2% w/w (30 ml) were foamed at room temperature in a graduated tube (3 cm diameter) for 3 min with Griffin & George stirrer at 200 rpm. Overrun was calculated as Foam Overrun (FO):

$$\text{FO}\ (\%) = [(\text{foam volume}\ (\text{ml}) - 30\ (\text{ml}))/30\ (\text{ml})] \times 100 \quad (2)$$

The data reported are means of at least two replicates. The error was 10%.

2.4.2. Foam drainage

The volume of liquid drained to the bottom of the graduated tubes and foam height decrease related to collapse, were recorded as a function of time. The following empirical mathematical model was applied to fit the drainage over time [4]:

$$v(t) = Vt^n/c + t^n \quad (3)$$

where: $v(t)$ was the volume drained at time t; V *is* the maximum volume drained; n was a constant related to the sigmoid shape of the curves; and c was a constant related to drainage half time by $c^{1/n}$. The rate constant for drainage (k_{dr}) was calculated as:

$$k_{dr} = n/Vc^{1/n} \quad (4)$$

The data reported are means of at least two replicates. The error in k_{dr} was 11%.

2.4.3. Foam collapse

The decrease of foam volume (V) as a function of time (foam collapse) was described by the time required to start the collapse, (t.lag) and the time required to decrease the height of the foam in 10 ml, (collapse time).

The data reported are means of at least two replicates. The error was 10%.

2.5. High-intensity ultrasound (HIUS) treatment

Solutions of SPI were sonicated for 5, 10, 15 and 20 min using an ultrasonic processor Vibra Cell Sonics, model VCX 750 (maximum net power output: 750 W) at a frequency of 20 kHz, 4.27 ± 0.71 W and an amplitude of 20% without any booster. A 13 mm high grade titanium alloy probe threaded to a 3 mm tapered microtip was used to sonicate 10 ml of solution at 6% wt/wt. Samples contained into glass test tubes were, in turn, immersed into a glycerine-jacketed circulating constant temperature cooling bath at 0.5 °C to dissipate most of the heat produced during sonication and 75, 80 and 85 °C for temperature combined treatments (Polystat, Cole-Parmer).

2.6. Dynamic light scattering measurements

Dynamic light scattering (DLS) experiments were carried out in a Dynamic Laser Light Scattering instrument (Zetasizer Nano-ZS, Malvern Instruments, Worcestershire, United Kingdom) provided with a He–Ne laser (633 nm) and a digital correlator, Model N3600. The average value and standard deviation of ten measurements per sample is reported. The particle size is calculated from the translational diffusion coefficient by using the Stokes Einstein equation:

$$d_h = kT/3\pi\rho\eta D \quad (5)$$

where, d_h is the hydrodynamic diameter; D the translational diffusion coefficient; k the Boltzmann's constant; T the absolute temperature and η the viscosity. Protein solutions were filtered by 0.45 μm previous to the measurement and intact samples were also measured by this technique.

2.7. Surface film balance

Measurements of the variations of surface pressure (π) with the molecular area (A) were completed at the air–water interface with an automated KSV Langmuir mini-trough (KSV Instruments Ltd., Helsinki, Finland), with a working surface area of 2.43×10^{-2} m^2. The surface pressure was measured with a Wilhelmy plate with an accuracy of ±0.1 mN/m. The system is enclosed in order to minimize water evaporation and to avoid external contaminations. The subphase in the trough was Milli-Q water (ultrapure water which purification processes involve successive steps of filtration and deionization to achieve a purity expediently characterized in terms of resistivity (typically 18.2 MΩ cm at 25 °C), at pH = 7.0 and all the measurements were performed at constant temperature (20 ± 1 °C) by circulating water from a thermostat. It was used the Trurnit's spreading method [19] for the preparation of a spread monolayer of protein, as it has been proved to be a widely used technique that ensured better results for the quantitative spreading of globular proteins at the air–water interface [20]. The barriers were closed at a constant rate of 10 mm/min, which is the highest value for the compression rate at which the corresponding isotherms were reproducible. Aliquots of aqueous protein solutions 8.1×10^{-4} mg/μl were spread on the interface. At least five isotherms were measured by using new aliquots.

In order to avoid the effect of possible impurities in all these surface measurements it was ensured that all materials and equipment were clean. By this way, it was checked the cleanliness of the subphase by measuring the surface tension of the aqueous subphase without protein, obtaining a negligible surface pressure rise (π less than 0.3 mN/m) when compressing the barriers.

As indicated by Rodríguez Niño et al. [21] the elasticity of the monolayer can be calculated from the slope of the π–A isotherm from Eq. (6):

$$E = -A(\mathrm{d}\pi/\mathrm{d}A) \tag{6}$$

where $\mathrm{d}\pi/\mathrm{d}A$ represents the slope for each step of the π–A isotherm and A is the average area corresponding to this slope. This is the elasticity at zero deformation rate. This monolayer elasticity is a measure of the film resistance to a change in area; higher values of E indicate the existence of a strong cohesive interfacial structure [22].

2.8. Statistical analysis

The model goodness-of-fit was evaluated by the coefficient of determination (R^2) and the analysis of variance (ANOVA), using Statgraphics Plus 3.0 software.

3. Results

3.1. Foaming properties after HIUS treatment

It was studied the effect of time of HIUS treatment from 5 to 20 min at room temperature on SPI foaming properties. The foaming capacity (FC) of the untreated soy protein was 153.3% which increased significantly at higher treatment times. During the first 5 min of treatment the FC increased by 62% respect to SPI, following a slight increase up to 75% at 20 min of sonication. Thus, it was decided to run all the studies at 20 min, where it was more pronounced the HIUS effect.

Regarding the foam stability (drainage and collapse) it was not observed any significant changes after HIUS treatment, although a slight increase in the drainage velocity at 5 and 15 min was observed.

Fig. 1 shows the foaming capacity (FC) of SP after 20 min of HIUS treatment at room temperature and at 70, 80 and 85 °C. In addition it is also shown the FC of only heat treated SPI.

In can be seen that the thermal treatment without HIUS, increased slightly the FC of SPI. The small difference could be attributed to the fact that SPI was previously heat treated; then further heat treatment did not modify significantly the protein structure which could influence the FC.

However, when the heat treatment was applied together with HIUS, the FC increased to 240% at every temperature studied (70, 80 and 85 °C). These values were higher than those obtained by HIUS at room temperature (202%).

When analyzing the foam stability parameters (Tables 1 and 2) only slight changes were observed in the lag time for drainage for the combined treatments, or the heated samples as well as an increase of the drainage velocity for HIUS treated (Table 1). It could be also seen a much higher collapse time for the samples heat treated at 80 and 85 °C (Table 2), that means their foams became more stable against collapse time.

Similar results were obtained by Nicorescu et al. [23]. They compared the effect of thermal treatments applied in typical industrial conditions on the foaming properties, by whipping method, of whey protein isolate (WPI at 80–100 °C, 2% w/w) and egg white proteins (EWP at 60–80 °C, 10% w/w) under dynamic conditions using a tubular heat exchanger. For WPI, statistical analysis showed that only a heat treatment at 90 °C or 100 °C seemed to slightly impair the foamability of native proteins. Conversely, overrun increased slightly with heat treatment of the EWP solutions in comparison to native proteins, but no significant differences in the overrun could be found between the different treatments applied. In other way, the thermal treatments improved significantly the stability of WPI and EWP foams but stability always passed through a maximum as a function of the intensity of heat treatment.

Moreover, the results obtained in the current work showed a synergistic effect between HIUS and temperature treatment. It was shown in previous studies that the impact of HIUS on proteins modification can be improved by increasing the temperature of the sample [24]. The authors demonstrated that ultrasound penetration can be enhanced by heat because of a viscosity decrease.

When comparing these results to that from the original native SPI foams, which showed a FC around 100% at the same experimental conditions [19]. It can be deduced that the treatment that induced the highest increase of FC was that with HIUS at 80 °C, where it could be reached a value of FC that was 144% higher than that corresponding to SPI.

3.2. Particle size distribution

Fig. 2 shows the particle size distribution (intensity (%) and volume (%)) for SPI treated with HIUS at room temperature, heat treated at 80 °C and treated by HIUS at 80 °C. In all cases studied, the curves presented a polymodal distribution with a marked peak at values above 100 nm (Fig. 2a). Similar results were obtained at the other temperatures (data not shown). The HIUS treatment at room temperature provoked a shift in the particle size distribution to lower diameters. It can be also seen that the sample only heat treated at 80 °C showed a major peak at 200 nm, whereas, when SPI was HIUS simultaneously treated, the value of this peak decreased and another peak at 30 nm appeared.

The volume particle size distribution (Fig. 2b) shows that most of the particles presented diameters less than 100 nm. Thus the number of the particles having size above 100 nm in Fig. 2a is negligible. It is important to note that when analyzing the volume distribution, the relationship between two populations identical in number, is 1:1000. When analyzing the intensity size distribution

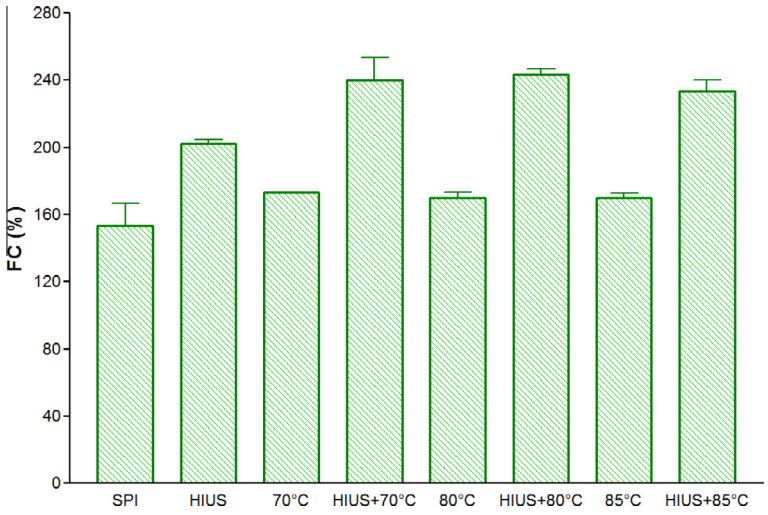

Fig. 1. Foaming capacity (FC) for treated samples.

Table 1
Drainage Stability parameters for SPI foams at different HIUS and temperatures treatments. Different letters between treatments indicate a significant difference at $P < 0.05$.

Treatment	Lag time for drainage (min) *	k_{dr} (ml min)$^{-1}$ *
SPI	1.5 ± 0.1^{ab}	$(8.7 \pm 0.4)10^{-3a}$
HIUS	0.8 ± 0.5^{a}	$(10.3 \pm 0.5)10^{-4ab}$
70 °C	1.5 ± 0.1^{ab}	$(15.4 \pm 1)10^{-3c}$
HIUS-70 °C	2.5 ± 0.1^{c}	$(8.8 \pm 1.8)10^{-3a}$
80 °C	1.5 ± 0.1^{ab}	$(13 \pm 0.1)10^{-3bc}$
HIUS-80 °C	2.5 ± 0.1^{c}	$(7.5 \pm 0.2)10^{-3a}$
85 °C	1.5 ± 0.1^{ab}	$(14 \pm 4.1)10^{-3c}$
HIUS-85 °C	2 ± 0.7^{bc}	$(8.5 \pm 0.4)10^{-4a}$

* Mean ± SD of at least three replicates, independently HIUS treated.

Table 2
Collapse Stability parameters for SPI foams at different HIUS and temperatures treatments. Different letters between treatments indicate a significant difference at $P < 0.05$.

Treatment	Lag time for collapse (min) *	Collapse time (min) *
SPI	7.2 ± 3.1^{cd}	170 ± 28^{a}
HIUS	2.8 ± 0.6^{ab}	180 ± 42^{a}
70 °C	2 ± 0.7^{a}	150 ± 14^{a}
HIUS-70 °C	3.5 ± 0.1^{ab}	145 ± 21^{a}
80 °C	4 ± 1.5^{ab}	>4 h
HIUS-80 °C	10 ± 0.2^{d}	135 ± 22^{a}
85 °C	2 ± 0.7^{a}	>4 h
HIUS-85 °C	5.5 ± 0.1^{bc}	125 ± 17^{a}

* Mean ± SD of at least three replicates, independently HIUS treated.

the ratio between the particles is 1:1,000,000, as the intensity of the scattered light is proportional to diameter 6 (Rayleighs approximation).

Most of the particles in SPI had a size at around 7 nm, which was decreased by HIUS treatment at room temperature (peak at 5 nm) as it was reported for other proteins [25]. The heat treatment at 80 °C strongly increased the size of the particles because of heat aggregation (peak above 20 nm). However, HIUS at 80 °C resulted (Fig. 2b) in a population at above 20 nm (similar to that obtained at 80 °C) and a lower size population at 2.6 nm.

Therefore, the combined treatment at high temperatures led to a decrease of the particles size caused by the rupture of the previously formed aggregates. The chances of being attacked by the cavitation energy rise with increasing the molecular weight of the different species. Thus, the aggregates that were formed by heat could be broken into small particles by HIUS.

Some authors [26] studied high-intensity ultrasounds applications for 5, 20 or 40 min on soy protein isolate particles size distribution. They observed that the volume–mean diameter (D_{43}) of soy protein dispersions decreased significantly during the first 20 min, while remaining unchanged from 20 to 40 min, suggesting that longer ultrasound treatment did not cause further changes in the particle size of soy protein dispersions under their experimental conditions.

3.3. Correlation between foaming capacity and particle size

There existed few works that relates the foaming properties with the particle size of protein aggregates. So, in order to evaluate the possible relationship between FC and the particle size of SPI samples, it was first evaluated the mean hydrodynamic diameter from each polymodal particle size distributions as Z_{av}.

It is shown in Fig. 3 the value of Z_{av} for the different SPI samples. It can be seen two well-differentiated groups: that of the heat treated SPI, which presented values of Z_{av} of approximately 100 nm, and other group corresponding to the samples that were simultaneously HIUS treated, with values of Z_{av} of approximately 63 nm. This value was similar to that obtained when HIUS was applied at room temperature. This suggests that the rupture of the protein aggregates by sonication is a dominant mechanism over the aggregation effect as a consequence of the heat treatment. This behavior was also observed when heating the whey protein isolate (WPI) at 7.5% w/w at a higher temperature (85–93 °C) upon sonication [14].

Fig. 4 shows the impact of the mean hydrodynamic diameter (Z_{av}) of SPI filtered samples on FC.

It can be deduced that FC was increased with decreasing Z_{av}. Two regions may be defined by the intersection of the slopes corresponding to the lower and the higher particle size-dependence. A critical value of Z_{av} at 70 nm was found to delimit these two regions. However, as the foams were prepared with unfiltered SPI solutions, it was also evaluated the Z_{av} of unfiltered samples in order to correlate these values with the FC (Fig. 5). The same tendency was observed, as FC increased with decreasing Z_{av}. However, the critical value of Z_{av} was observed at 110 nm. Thus, it can be conclude that a decrease of particle size below 110 nm strongly increases FC of SPI. The samples presenting Z_{av} minor to 110 nm were all HIUS treated.

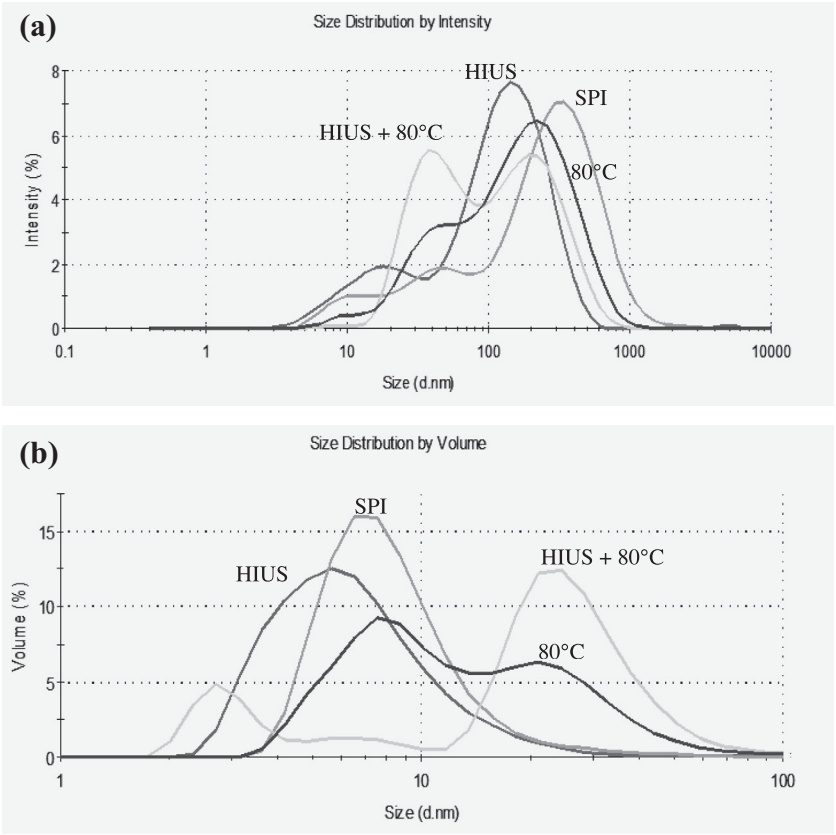

Fig. 2. Particle size intensity (%) (a) and volume (%) (b) distributions for filtered treated samples by 0.45 μm.

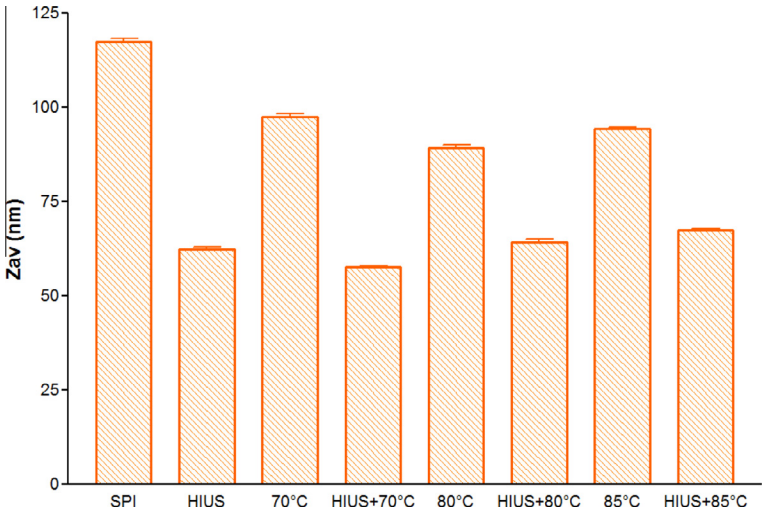

Fig. 3. Mean hydrodynamic diameter (Z_{av}) for treated samples filtered by 0.45 μm.

The intensity size distributions of unfiltered samples corresponding to each treatment were analyzed so as to identify the particles populations responsible of the observed behavior of FC (Fig. 5). It was observed for untreated SPI a very important peak at 5500 nm, which also appeared when heating SPI. However, when HIUS were applied, the biggest populations disappeared, corresponding with a marked increase on FC. Thus, even in a low proportion, the populations with a higher particle size could influence the foaming properties performance.

Similar results were observed by Nicorescu et al. [23] working with whey protein isolate (WPI). They studied the influence of dynamically heat-induced aggregates as a function of the thermal treatment by using a bubbling technique. The aim of this work was to determine the interplay between the size/shape/proportion of the heat-induced aggregates and the properties of protein foams (formation and stability). Protein aggregates were shown to slow down significantly the foam formation. However, the rate of foam formation remained almost unchanged for wet foams when the amount of insoluble aggregates was bellow to 5% and when their size remained lower than 100 μm. Similarly, protein aggregates did not seem to affect the kinetics destabilisation of wet foams, regardless of amount, size, shape and proportion as observed in this work.

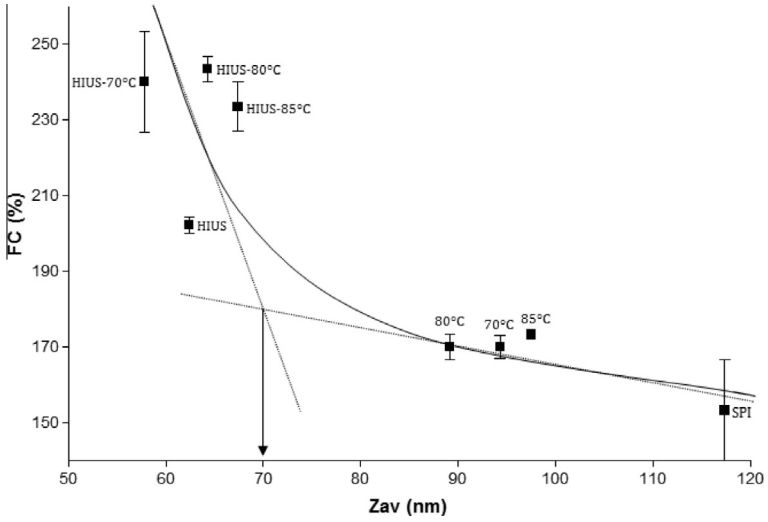

Fig. 4. Foaming capacity (FC) as a function of mean hydrodynamic diameter (Z_{av}) for SPI, filtered treated samples by 0.45 μm.

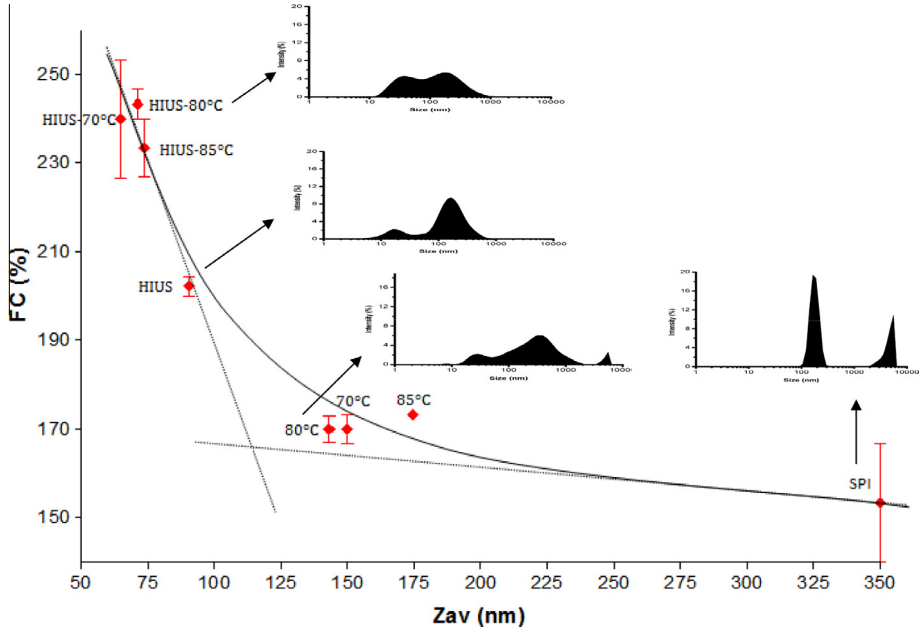

Fig. 5. Foaming capacity (FC) as a function of mean hydrodynamic diameter (Z_{av}) for SPI, without filter use.

3.4. Structural characteristics of spread monolayers at the air–water interface

The structural characteristics of SPI treated films were studied through the surface pressure-molecular area isotherms (π–A) (Fig. 6). It was checked the quantitative spreading protein at the air–water interface (data not shown) by using several spreading solutions at different protein concentrations [27].

Fig. 6 shows the π–A isotherms for the different SPI samples. The π–A isotherms are similar and parallel to each other (it could be possible to merge these isotherms into one practically identical isotherm), until the surface pressure reached a transition point at approximately 14 mN/m (related to a change into a more condensed state of the protein film at the air–water interface [28]. After this moment the amino acid segments change their structure at the air–water interface, that is, before reaching this transition they existed as trains with all amino-acid segments located at the interface and at higher surface pressures (after the transition) the amino-acid segments are extended into the underlying aqueous solution and adopt the form of loops and tails. Carrera Sanchez et al. [29] also found a change of the protein film structure at approximately 19–20 mN/m for soy protein fractions (7S, 11S and 11S + DTT) at pH 8.0.

It can be deduced from these experiments (Fig. 6) the effect of the different treatments that were applied to the SPI. Isotherms displaced in the π–A axis depending on the applied treatment. There exists a shift of the π–A isotherm to higher values of area when HIUS was applied, indicating that the protein is more expanded at the air–water interface because of the application of HIUS. It occurs because protein is more flexible, as it can unfold so as to assume the most favorable thermodynamic configuration [30]. However, when only heat was applied (80 °C), the contrary effect was observed as the isotherm shifted to lower values of area. It shows that the protein film is more condensed and it could occur because of the heat-induced interfacial aggregation [21,31]. The SPI treated by HIUS at 80 °C presented behavior close to that obtained

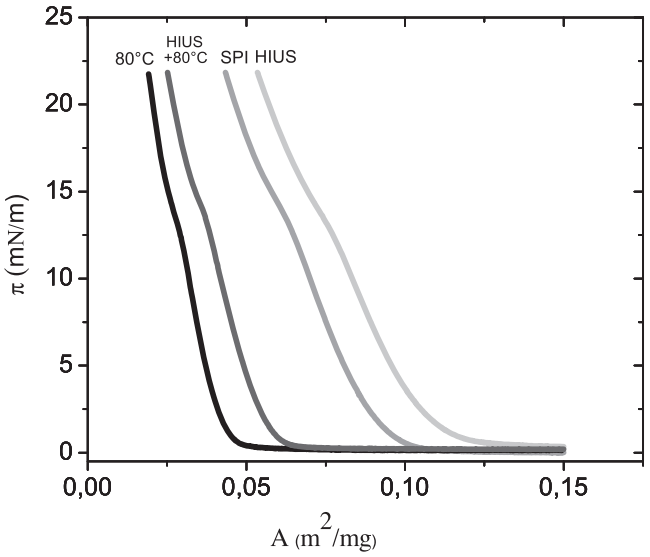

Fig. 6. Surface pressure isotherms *vs*. molecular area for treated samples.

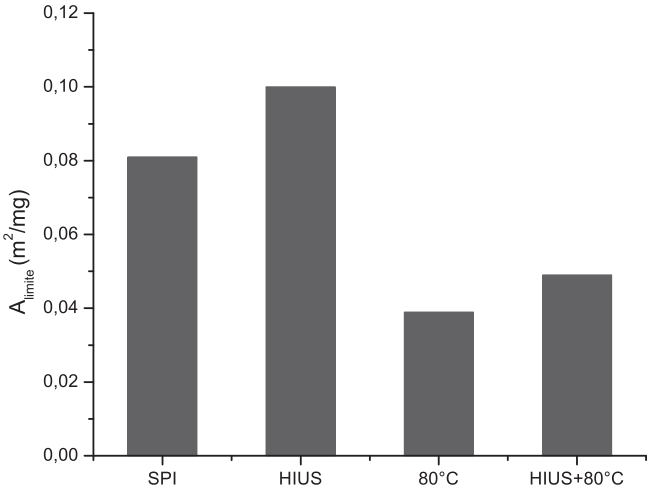

Fig. 7. Molecular limit area for SPI treated samples.

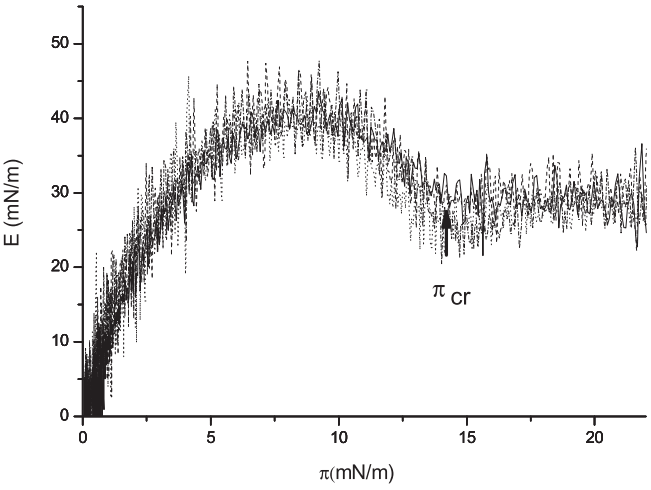

Fig. 8. Interfacial elasticity *vs*. surface pressure for SPI: SPI (---); HIUS (....) HIUS + 80 °C (-.-.-.-).

from the application of temperature, although the π–A isotherm shifted to the left in a lower extension.

In addition, the values of the limiting area (A_{lim}) could also be obtained from the π–A isotherms for the different systems (Fig. 7). The limiting area is the area in the most condensed region of the protein film extrapolated to $\pi = 0$, as indicated by Rodríguez Patino et al. [32]. This parameter is a measure of the interfacial area occupied by protein residues at the air–water interface. A decrease of limiting area indicates a more condensed structure of film [21,28]. It can be observed the lowest limiting area for the heat treated SPI (80 °C), which suggest the highest condensation degree of the protein at the air–water interface. However, an opposite result was observed when HIUS was applied on SPI, which denote a more expanded structure of the adsorbed protein.

Related to the mean particle size characterized by the Z_{av} (Fig. 3), it can be seen that the lower was the Z_{av}, the more expanded was the protein at the interface, which related with the foaming capacity improvement. Thus, it can be concluded that a more expanded structure of SPI with a better foaming performance of protein particles at liquid interfaces which can be achieved when lower particles sizes were obtained.

3.5. Elasticity of films

The elasticity (E) of the protein films was determined from the π–A isotherm as indicated previously [21]. Fig. 8 shows the change of E as a function of surface pressure π. All the SPI films showed a similar behavior. It can be observed a minimum of elasticity at similar values of the surface pressure (π_{cr} = 14–15 mN/m) that is associated with the configurational transitions in the interfacial structure of proteins from expanded to more condensed structures [33,21,34].

The maximum elasticity of films was apparent at about π = 10 mN/m just before the transition to a condensed structure.

Therefore, the interfacial elasticity of the protein films, was not affected by the different treatments applied to SPI nor to the size of particles, which probably accounts for by the unchanged foam stability (Tables 1 and 2).

4. Conclusions

The HIUS treatment improved the foaming capacity whereas the stability of the foams was not significantly modified. The ultrasounds showed a synergistic effect with the temperature on the foaming capacity of SPI. The foaming capacity increase exhibited a good correlation with the decrease of particle size of SPI, thus, it is the main factor that dominates this property. However, other factors could also contribute to increase the foaming capacity, as surface hydrophobicity.

Finally, the invariable stability of foams obtained was in accordance with interfacial studies through the rheological results of the interfacial films observed after the different treatments.

Molecular particle size of proteins, among other factors (protein structure, shape, charge, hydrophobicity, free sulfhydryl content and amino acid composition) determines the adsorption rate of the protein to the interface. The lower the particle size, the faster proteins can absorb to the liquid interface.

In many works, where the ultrasound technique was applied on proteins and the foaming properties were also studied, it was reported that foam stability did increase after this treatment. The ultrasound process homogenizes, disperses the proteins and partially unfolds them leading to foaming properties enhancement. However, some authors have also reported that, when using high frequency values, the foam stability was unchanged, as it was also observed in the present work.

HIUS technology can possibly improve the production processes to provide products with better characteristics and new functionalities in the food and bioprocessing industry, but its success relies both on the knowledge of the protein response and the expertise of its use. As it has not been tested yet large scale applications, experiments, starting from little amounts of sample, are true "starting points". On the other side, this development leads to the creation of environmentally friendly processes and compounds, emphasizing the role of ultrasound and food proteins into the so called "Green Chemistry".

Acknowledgments

This research was supported by Universidad de Buenos Aires (UBACYT 20020100200221), Agencia Nacional de Promoción Científica y Tecnológica (PICT 2008-1901) and Consejo Nacional de Investigaciones Científicas y Técnicas de la República Argentina.

References

[1] E. Dickinson, An Introduction to Food Colloids, Oxford University Press, Oxford, UK, 1992.
[2] P. Walstra, Overview of emulsion and foam stability, in: E. Dickinson (Ed.), Food Emulsions and Foams, Wagenigen, The Nederlands, 1988, pp. 242–257.
[3] J.E. Kinsella, Functional properties in foods, possible relationships between structure and function in foams, Food Chem. 7 (1981) 273–288.
[4] S. Utsumi, Y. Matsumura, Function relationships of soy proteins, in: S. Damodaran, A. Paraf (Eds.), Food Proteins and Their Applications, Marcel Dekker Inc, 1997.
[5] M. Liu, D.-S. Lee, S. Damodaran, Emulsifying properties of acidic subunits of soy 11S globulin, J. Agric. Food Chem. 47 (1999) 4970–4975.
[6] D.J. Carp, B.G. Bartholomai, A.M.R. Pilosof, A kinetic model to describe liquid drainage from soy protein foams over an extensive protein concentration range, Lebensm. Wiss. Technol. 30 (2) (1997) 253.
[7] S.H. Kim, J.E. Kinsella, Surface active properties of food proteins: effects of reduction of disulfide bonds on film properties and foams stability of glycinin, J. Food Sci. 52 (1987) 128–131.
[8] R.H. Chen, J.R. Chang, J.S. Shyur, Effects of ultrasonic conditions and storage in acidic solutions on changes in molecular weight and polydispersity of treated chitosan, Carbohydr. Res. 299 (4) (1997) 287–294.
[9] R. Eschette, D.P. Norwood, "Ultrasonic degradation of polysaccharides studied by multiangle laser light scattering", Presented as Poster Number RI-107 at the Annual March Meeting of the American Physical Society, Austin, TX, USA, March 3–7, 2003.
[10] Y. Iida, T. Tuziuti, K. Yasui, A. Towata, Control of viscosity in starch and polysaccharide solutions with ultrasound after gelatinization, Innovative Food Sci. Emerg. Technol. 9 (2) (2008) 140–146.
[11] N. Kardos, J.-L. Luche, Sonochemistry of carbohydrate compounds, Carbohydr. Res. 332 (2) (2001) 115–131.
[12] H.B. Liu, Effect of ultrasonic treatment on the biochemphysical properties of chitosan, Carbohydr. Polym. 64 (4) (2006) 553–559.
[13] J.P. Lorimer, Effect of ultrasound on the degradation of aqueous native dextran, Ultrason. Sonochem. 2 (1) (1995) S55–S57.
[14] L. Gordon, A.R. Pilosof, Application of high intensity ultrasounds to control the size of whey proteins particles, Food Biophys. 5 (2010) 203–210.
[15] B. Zisu, R. Bhaskaracharya, S. Kentish, M. Ashokkumar, Ultrasonic processing of dairy systems in large scale reactors, Ultrason. Sonochem. 17 (6) (2011) 1075–1081.
[16] D. Knorr, M. Zenker, V. Heinz, D. Lee, Applications and potential of ultrasonics in food processing, Trends Food Sci. Technol. 15 (5) (2004) 261–266.
[17] D.J. Carp, B. Bartholomai, P. Relkin, A.M.R. Pilosof, Effects of denaturation on soy protein–xanthan interactions: comparison of a whipping-rheological and bubbling method, Colloids Surf. B 21 (2001) 163–171.
[18] K.D. Martínez, C. Carrera Sánchez, J.M. Rodríguez Patino, A.M.R. Pilosof, Interfacial and foaming properties of soy protein and their hydrolysates, Food Hydrocolloids 23 (2009) 2149–2157.
[19] H.J.A. Trurnit, Theory and method for the spreading of protein monolayers, J. Colloid Sci. 15 (1960) 1–13.
[20] Carrera Sánchez et al., Soy globulin spread films at the air–water interface, Food Hydrocolloids 18 (2004) 335–347.
[21] M.R. Rodriguez Niño, C. Carrera Sánchez, J.M. Rodríguez Patino, Interfacial characteristics of-b-casein spread films at the air–water interface, Colloids Surf. B 12 (1999) 161–173.
[22] J. Maldonado-Valderrama, H.A. Wege, M.A. Rodríguez-Valverde, M.J. Gálvez-Ruiz, M.A. Cabrerizo-Vílchez, Comparative study of adsorbed and spread β-casein monolayers at the water–air interface with the pendant drop technique, Langmuir 19 (2003) 8436–8442.
[23] I. Nicorescu, C. Vial, E. Talansier, V. Lechevalier, C. Loisel, D. Della Valle, A. Riaublanc, G. Djelveh, J. Legrand, Comparative effect of thermal treatment on the physicochemical properties of whey and egg white protein foams, Food Hydrocolloids 25 (4) (2001) 797–808.
[24] M. Villamiel, P. Jong, Influence of high-intensity ultrasound and heat treatment in continuous flow on fat proteins, and native enzymes of milk, J. Agric. Food Chem. 48 (2000) 472–478.
[25] A. Jambrak, T.J. Mason, V. Lelas, L. Paniwnyk, Z. Herceg, Effect of ultrasound treatment on particle size and molecular weight of whey proteins, J. Food Eng. 121 (2014) (2014) 15–23.
[26] Hao Hu, Eunice C.Y. Li-Chan, Wan Li, Ming Tian, Siyi Pan, The effect of high intensity ultrasonic pre-treatment on the properties of soybean protein isolate gel induced by calcium sulfate, Food Hydrocolloids 32 (2013) (2013) 303–311.
[27] F. MacRitchie, Spread monolayers of proteins, Adv. Colloid Interface Sci. 25 (1986) 341–386.
[28] José Miñones Conde, Juan M. Rodríguez Patino, José Miñones Miñones Trillo, Structural characteristics of hydrolysates of proteins from extracted sunflower flour at the air–water interface, Biomacromolecules 6 (2005) 3137–3145.
[29] C. Carrera Sanchez, S.E. Ortiz, M.R. Niño, M.C. Añon, J.M. Patino, Effect of pH on structural, topographical, and dynamic characteristics of soy globulin films at the air–water interface, Langmuir 19 (2003) 7478–7487.
[30] D.G. Güzey, Interfacial properties and structural conformation of thermosonicated bovine serum albumin, Food Hydrocolloids 20 (5) (2006) 669–677.
[31] Elena V. Kudryashova, Antonie J.W.G. Visser, Jongh De, H.J. Harmen, Reversible self-association of ovalbumin at air–water interfaces and the consequences for the exerted surface pressure, Protein Sci. 14 (2005) 483–493.
[32] Juan M. Rodríguez Patino, Manuela Ruiz Dominguez, Julia De la Fuente Feria, The effect of sugars on monostearin monolayers, J. Colloid Interface Sci. 157 (1993) 343–354.
[33] Ana Lucero Caro, M. Rosario Rodríguez Niño, Juan M. Rodríguez Patino, The effect of pH on structural, topographical and rheological characteristics of β-casein-DPPC mixed monolayers spread at the air-water interface, Colloids Surf. A 332 (2009) 180–191.
[34] Virginie Martinet, Patrick Saulnier, Valérie Beaumal, Jean-Luc Courthaudon, Marc Anton, Surface properties of hen egg yolk low-density lipoproteins spread at the air–water interface, Colloids Surf. B 31 (2003) 185–194.